Received: 22 July 2022 | Revised: 27 July 2023 | Accepted: 7 August 2023

DOI: 10.1111/jbi.14709

Journal of Biogeography

WILEY

RESEARCH ARTICLE

Biogeographic barriers and historic climate shape the phylogeography and demography of the common gartersnake

Leonard N. Jones II[1,2] | Adam D. Leaché[2] | Frank T. Burbrink[3]

[1]Department of Ecology and Evolutionary Biology, University of Michigan, Ann Arbor, Michigan, USA

[2]Department of Biology, Burke Museum of Natural History and Culture, Seattle, Washington, USA

[3]Department of Herpetology, The American Museum of Natural History, New York, New York, USA

Correspondence
Leonard N. Jones II, Department of Ecology and Evolutionary Biology, University of Michigan, Ann Arbor, MI, USA.
Email: leonard.jones@gmail.com

Funding information
American Museum of Natural History; National Science Foundation, Grant/Award Number: 1600844

Handling Editor: Rayna Bell

Abstract

Aim: Current distributions of widespread North American (NA) species have been shaped by Pleistocene glacial cycles, latitudinal temperature gradients, sharp longitudinal habitat transitions and the vicariant effects of major mountain and river systems that subdivide the continent. Within these transcontinental species, genetic diversity patterns might not conform to established biogeographic breaks compared to more spatially restricted taxa due to intrinsic differences or spatiotemporal differences. In this study, we highlight the effects of these extrinsic variables on genetic structuring by investigating the phylogeographic history of a widespread generalist squamate found throughout NA.

Location: North America.

Taxon: Common gartersnake, *Thamnophis sirtalis*.

Methods: We evaluate the effects of major river basins and the forest-grassland transition into the Interior Plains on genetic structure patterns using phylogenetic, spatially informed population structure and demographic analyses of single nucleotide polymorphism data and address range expansion history with ecological niche modelling using locality and historic climate data.

Results: We identify four phylogeographic lineages with varying degrees of connectivity between them. We find discordant population structure patterns between sex-linked and autosomal loci with respect to the relationship between the central NA lineage relative to coastal lineages. We find support for southeast Pleistocene refugia where recent secondary contact occurred during the Last Glacial Maximum and evidence for both northern and southern refugia in western NA.

Main Conclusion: Our results provide strong evidence for a Pliocene origin for *T. sirtalis* in central-southeastern NA preceding its rapid expansion across the continent prior to middle Pleistocene climate-mediated lineage formation. We implicate major riverine networks within the Mississippi watershed in likely repeated westward expansion events across the Interior Plains. Finally, we corroborate prior conclusions that phenotypic differences between subspecies do not reflect shared evolutionary history and note that the degree of separation between inferred lineages warrants further investigation before any taxonomic revisions are proposed.

KEYWORDS
biogeography, demography, North America, phylogeography, Pleistocene, spatial population structure

1 | INTRODUCTION

North America (NA) comprises multiple ecoregions containing over 150 terrestrial habitat types (Bailey, 1995; Lobeck, 1948; Ricketts et al., 1999). Numerous phylogeographic studies have characterized the effects of major habitat boundaries and biogeographic breaks on intraspecific variation across the tree of life (Beheregaray, 2008; Calsbeek et al., 2003; Shafer et al., 2010; Zink, 2002). Within the temperate mixed forested regions of eastern NA (herein, Eastern Forest), the Atlantic Coastal Plain, Appalachian Highlands, the Apalachicola-Chattahoochee-Flint (ACF) River Basin, and Mississippi watersheds have served as barriers to gene flow in multiple floral and faunal populations (Soltis et al., 2006). Throughout the temperate forests of the Pacific Coast and Northwest, Miocene mountain chain uplifts and Pleistocene glacial cycles have been implicated in shaping contemporary genetic diversity (Shafer et al., 2010; Soltis et al., 1997; Steele & Storfer, 2006). The Interior Plains separates these two regions and represents a sharp shift in vegetation type and average precipitation, and as a result, this region is among the most well-studied biogeographic breaks for multiple wide-ranging species and populations that span it (Reding et al., 2012, 2021; Rising, 1983; Swenson & Howard, 2005).

In wide-ranging species, the relative contribution of ecological adaptation to different biomes, historical isolation followed by secondary contact, and selection acting upon intraspecific lineages can be difficult to distinguish (Burbrink, Bernstein, et al., 2021; Burbrink, Gehara, et al., 2021; Edwards et al., 2016; Fujita et al., 2012; Harris et al., 2018; Leaché et al., 2009; Riddle, 2016). Additionally, these species may exhibit continuous variation correlated with spatial separation (IBD; Bradburd et al., 2013; Wright, 1943) and/or be subject to asynchronously timed geological and climatic processes in different biogeographic regions (Chardon et al., 2020). Phylogeographic comparisons between co-distributed taxa can help clarify drivers of demographic and evolutionary patterns, but similar diversification patterns caused by different processes can confound identification of the processes underlying divergence (Irwin, 2002; Soltis et al., 2006). Therefore, for single species, understanding historical demography, population structure, phylogeny and ecology is important for characterizing sources of variation within.

Widespread vertebrate ectotherms are particularly valuable systems for understanding the role of continental scale habitat transitions and vicariance due to their narrower environmental constraints (Deutsch et al., 2008; Hewitt, 1996; Moritz et al., 2012; Wiens, 2004) and lower dispersal distances compared to mammalian and avian systems (Buckley & Jetz, 2007; Rolland et al., 2018). Recent work has characterized the role of forest-grassland habitat transitions in ecological diversification of amphibian and reptile species (Austin et al., 2004; Burbrink et al., 2016; Burbrink, Bernstein, et al., 2021; Burbrink, Gehara, et al., 2021; Finger et al., 2022; Myers et al., 2020; Rissler & Smith, 2010). Few NA vertebrate ectotherms exhibit distributions that comprise the entire longitudinal extent of the continent (Austin et al., 2004; Burbrink et al., 2008; Fontanella et al., 2008; Leaché & Reeder, 2002; Lee-Yaw et al., 2008), making these transcontinental species particularly valuable for testing hypotheses concerning the roles of ecological gradients, vicariance and glacial cycles in intraspecific divergence.

The common gartersnake *Thamnophis sirtalis* is the most widely distributed terrestrial vertebrate ectotherm in NA and one of the most well-studied snakes in the world regarding behaviour, ecology and adaptation (Brodie, 1968; Feldman et al., 2010; Garland, 1988; Gregory, 1984; Mason, 1993: 199; Perry et al., 2018; Ralph Gibson & Bruce Falls, 1979; Rossman et al., 1996; Shine et al., 2001). A consummate riparian generalist, the range of *T. sirtalis* (Figure 1) spans multiple ecoregions and biogeographic barriers known to shape the genetic structure within many disparately related taxa (Avise, 2000; Brunsfeld et al., 2001; Soltis et al., 2006). Phylogenetic studies of the genus *Thamnophis* (Guo et al., 2012; Hallas et al., 2022; McVay et al., 2015; Nuñez et al., 2023) have stabilized taxonomy and generally support a middle Miocene origin in southern NA followed by divergence into a widespread northern clade containing *T. sirtalis* (Northern Mexico, contiguous US, Canada) and a southern clade occurring within the Mexican Transition Zone. Phylogeographic studies within the northern clade have identified Pleistocene signatures in contemporary population structure in central and western NA (Allen, 2005; Hallas et al., 2021). *T. sirtalis* is perhaps most well-known for its extensive regional phenotypic variation—12 subspecies defined by colour patterns associated with geography are currently recognized (Rossman et al., 1996; Uetz et al., 2019). Half of these occur along the Pacific Coast, a comparatively small portion of its range that *T. sirtalis* is hypothesized to have recolonized at the end of the Pleistocene, ~10 kya (Janzen et al., 2002). Prior population genetic and phylogeographic studies using mtDNA from western (Hague et al., 2017, 2020; Janzen et al., 2002; Ridenhour et al., 2007) and central NA populations (Placyk et al., 2007) suggest vicariant history and recent expansion from Pleistocene refugia, rather than shared ancestry, explain the observed diversity. Unfortunately, there is no assessment of population structure in south-central and southeastern NA, where studies of other terrestrial ectotherms have revealed cryptic signatures of intraspecific divergence shaped by the ACF and Mississippi basins and the Atlantic Coastal Plain demarcating peninsular Florida populations from those of the mainland (Burbrink, 2002; Burbrink et al., 2000; Burbrink et al., 2008, 2016; Fontanella et al., 2008; McKelvy & Burbrink, 2017). Due to their semiaquatic nature in parts of their distribution (Rossman et al., 1996), genetic diversity within *T. sirtalis* might not conform

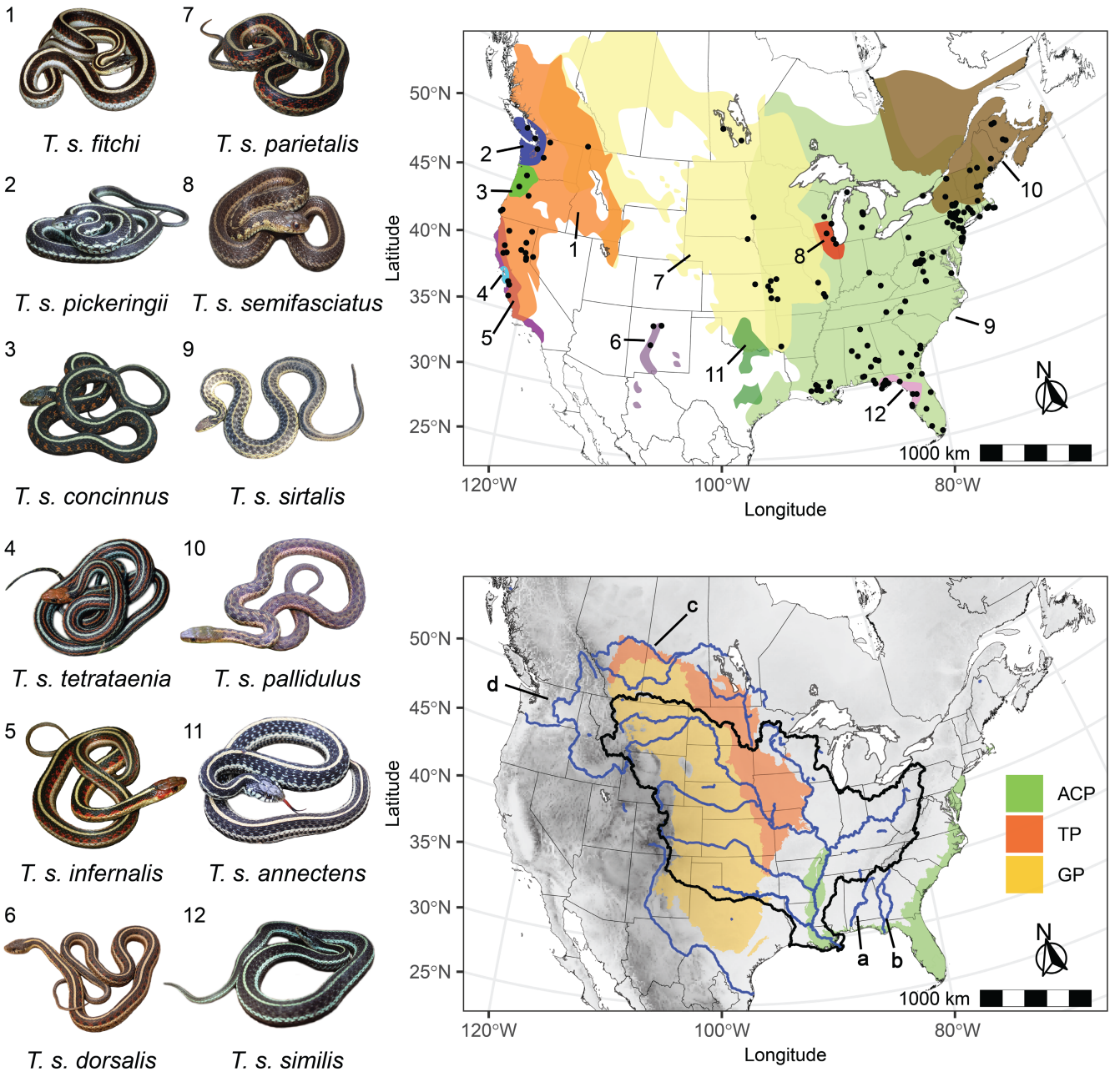

FIGURE 1 Distribution of the common gartersnake *Thamnophis sirtalis* (Top) and proposed biogeographical factors (Bottom) influencing its westward expansion. Unique subspecies ranges adapted from Rossman et al. (1996) and the IUCN database and modified with spatial analyses of museum records downloaded from GBIF. Bottom map shows the Southeast Atlantic Coastal Plain ecoregion (light green, ACP), the Alabama River (a) and the Apalachicola-Chattahoochee-Flint River Basin (b), which have been implicated in population genetic substructure in multiple flora and fauna species in the southeastern United States. Major rivers of the Mississippi watershed (outlined in black), the Saskatchewan River (c) and the Columbia River (d) likely facilitated westward expansion across the northern Great Plains (dark yellow, GP) and Temperate Prairies (dark orange, TP) of central North America, which represent comparatively less suitable habitat for *T. sirtalis*. Photo credits: (1, 4, 5) Gary Nafis (californiaherps.com), (2) Jonathan Hakim (iNaturalist), (3) J. Maughn (flickr), (6) James N. Stuart, (7) Jake Scott, (8) timoteo_b (iNaturalist), (9) hb2000 (iNaturalist), (10) J. D. Wilson (iNaturalist), (11) John Williams (iNaturalist), (12) Robert Simons (iNaturalist).

to patterns shaped by riverine barriers. Furthermore, given the prevalence of shallow introgression observed within and between multiple *Thamnophis* species to date (De Queiroz & Lawson 1994; Fitzpatrick et al., 2008; Kapfer et al., 2013; Placyk et al., 2007), it remains unclear how uniform these phylogeographic patterns are across the genome. Recent work suggests sex-linkage may drive lower-than-expected heterozygosity in *T. sirtalis* populations under regional selection (Gendreau et al., 2020).

Here we present the rangewide phylogeography of *T. sirtalis*. From phylogeographic and demographic analyses of mtDNA and

genome-wide single nucleotide polymorphism (SNP) data, we identify biogeographic lineages and genomic regions of disagreement among the relationships of these lineages. We use species distribution modelling to quantify environmental niche differentiation between these lineages and assess which if any habitat shifts and climactic gradients might explain lineage differentiation across the range of *T. sirtalis*. From previous work, we hypothesize a southeast/south-central origin for *T. sirtalis* and seek to characterize the tempo and mode of its westward expansion out of the Eastern Forest and across the Interior Plains. Specifically, we ask if (1) in the east, *T. sirtalis* shares the same divergence patterns shaped by intermontane systems, the ACF, and Atlantic Coastal Plain-Eastern Forest divide as other vertebrate terrestrial ectotherms (2) if the major rivers of the Mississippi watershed have acted as vicariant barriers between putative lineages or facilitators of westward expansion. Finally, we address congruence between the inferred lineages and current subspecies taxonomy.

2 | MATERIALS AND METHODS

2.1 | Sampling and data collection

We assembled tissues from localities spanning the entire *T. sirtalis* distribution (Figure 1) from field sampling and museum collections (Table S1). In part, due to their questionable validity and range limits, *T. sirtalis* subspecies are often not explicitly identified in museum collections. Where possible, we designated putative subspecies based on localities where only one taxon is known to occur. We isolated and qualified genomic DNA using NaCl extraction and gel electrophoresis followed by a Qubit dsDNA BR assay (Life Technologies, Inc.).

We generated ddRADseq libraries for 212 samples following Peterson et al. (2012). We digested 500–1000 ng DNA with restriction enzymes *Sbf*I and *Msp*I and ligated unique barcodes to individual samples. Barcoded samples were then pooled together in groups of up to eight individuals, and pools were size selected for 415–515 bp fragments with a Pippin Prep system (Sage Science, Inc.). The resulting products were amplified using a Phusion High Fidelity Taq polymerase kit (New England Biolabs, Inc.) with Illumina primers that introduce unique multiplexing indices to each pool upon amplification. Pools were amplified for 30 cycles at 51°C annealing temperature. Final libraries were purified using Ampure XP beads and fragment length distribution and molarity were calculated with an Agilent 2200 Tapestation. Libraries were sequenced across three Illumina HiSeq 4000 lanes (50-bp single-end reads) at UC Berkeley QB3 facility.

For 67 individuals, we sequenced a 812 bp fragment of mitochondrial locus cytochrome *B* (*cytB*) using primers from previous studies (L14910: 5′-GAC CTG TGA TMT GAA AAA CCA YCG TTG T-3′; H16064: 5′-CTT TGG TTT ACA AGA ACA ATG CTT TA-3′, Burbrink et al., 2000; De Queiroz et al., 2002). We supplemented these data with previously published *cytB* sequences for 32 congeners and other natricid species (Alfaro & Arnold, 2001; De Queiroz et al., 2002; De Queiroz & Lawson, 2008) (Table S2). We edited and aligned the resulting dataset with `Geneious` 5.1.7 (`Geneious` 5.1.7, http://www.geneious.com) under global alignment default parameters (Cost matrix: 65% similarity; gap open penalty: 12; gap extension penalty: 3).

2.2 | ddRADseq bioinformatics

We processed raw Illumina reads using `stacks` 2.5 (Rochette et al., 2019) `ref_align` pipeline against the chromosome level assembly of the *T. elegans* genome (Assembly: GCA_009769535). We demultiplexed and filtered reads with the `process_radtags` function and discarded reads with a quality score limit of <20 and/or a single base pair difference in adapter and barcode sequences. We retained loci present in 80% of the individuals of a putative population with the '`populations`' function, following the *r80* method outlined as best bioinformatic practice (Paris et al., 2017). We collected one SNP per locus and used the 'ordered-export' flag to ensure the absence of duplicate SNPs resulting from overlapping loci. After removing samples with high amounts of missing data/low read counts, we retained genomic data for 195 individuals representing 10 subspecies (Table S1). We generated additional datasets with *T. sirtalis* samples for which both mtDNA and SNP data were generated ($N = 59$) for nuclear versus mtDNA tree topology comparison, and a dataset for species tree estimation and demographic analysis with no missing data and four individuals per population ($N = 16$) to accommodate computational constraints.

2.3 | Population identification and migration modelling

In heterogametic species, sex chromosomes have lower effective population sizes than autosomes due to lower copy number, and consequently, observed variation among them is more sensitive to the effects of sex-biased processes and historic demographic changes (Van Belleghem et al., 2018). Like most snakes, *T. sirtalis* has a ZW sex determination system (females are ZW, males are ZZ) (Baker et al., 1972; Vicoso et al., 2013). To account for differences in population structure across the genome, we generated separate datasets for loci that mapped to autosomes and the Z chromosome. We then identified the number of roughly detectable clusters from the Z, autosomal and total datasets using principal components analysis (PCA) in `adegenet` 2.1.1 (`glpca` function) (Jombart, 2008). We estimated pairwise F_{ST} (Weir & Clark Cockerham, 1984) and inbreeding coefficients (F_{IS}) for all population pairs and additional genetic diversity measures (observed heterozygosity [H_O], observed genetic diversity [H_S], overall genetic diversity [H_T]) for each population and dataset with `hierfstat` (Goudet, 2005).

2.4 | Ancestry and gene flow estimation

We used TESS3r (Caye et al., 2016, 2018) to estimate ancestry in the total dataset. This approach incorporates geographic weighting of sample pairs into a least-squares optimization to determine the number of ancestral clusters that best explains genetic variation across the sampled space. Using the total SNP dataset, we estimated ancestry coefficients under default parameters for *K* values 1:10 with 20 replicates each and determined the appropriate *K* value using cross-validation.

We identified geographical regions of depressed migration rates with EEMS (Petkova et al., 2016). We constructed a coordinate file following the outer limits of the *T. sirtalis* distribution (Rossman et al., 1996). We calculated a dissimilarity matrix using PLINK 1.9 (Purcell et al., 2007). We analysed the SNP data with RUNEEMS_SNPS under four replicate analyses with a Markov chain Monte Carlo length of 5,000,000 and a burn-in of 1,000,000. We assessed convergence of the runs and visualized the combined results using EEMS'reemsplots2.

2.5 | Rangewide gene tree estimation and phylogenetic relationships

We estimated divergence times for *T. sirtalis* from *cytB* in BEAST 1.10 (Suchard et al., 2018). The high evolutionary rate, haploidy and near-zero recombination rate of mitochondrial loci preserve their value alongside multilocus markers generated from high throughput sequencing methods, particularly for identifying incomplete lineage sorting. We time-calibrated the tree using the earliest known *Thamnophis* fossil from the Medial Barstovian (13–14.5 Mya; Holman, 2000) and constrained the clade age of *Thamnophis* to a normal prior distribution (mean = 14, SD = 1) following previous studies (McVay et al., 2015; Wood et al., 2011). We selected the GTR+Γ+I substitution model using Bayesian information criterion in JModelTest2 (Darriba et al., 2012) and ran the analysis with a relaxed lognormal clock for 7,000,000 iterations sampling every 1000 steps. We ran two identical analyses with different random starting seeds and combined with LogCombiner and discarded the first 10% as burn-in. We checked parameter estimates for convergence with Tracer 1.7.1 (Rambaut et al., 2018).

We analysed the autosomal and Z-linked SNP datasets with IQ-TREE2 (Minh et al., 2020). We first used ModelFinder (Kalyaanamoorthy et al., 2017) to find the best fit model for the data by Bayesian information criterion, and then estimated maximum likelihood trees with 1000 ultrafast nonparametric bootstrap (Hoang et al., 2018) replicates under the GTR+F+ASC+R3 and GTR+F+ASC+R2 models for the autosomal and Z-linked datasets, respectively.

2.6 | Species tree estimation

We estimated species trees using SNAPP (Bryant et al., 2012) in BEAST 2.6 (Bouckaert et al., 2014), which generates the species tree directly from biallelic SNP data, and BPP 4.1 (Flouri et al., 2019), which infers species trees from multiple-sequence alignments. While we anticipated similar topologies from both coalescent approaches and acknowledge that both models can be biased by gene flow, IBD and sampling scheme (Mason et al., 2020; Stange et al., 2018), topological agreement between methods using full RAD loci (BPP) and SNPs (SNAPP) will provide evidence that the bifurcating topology is likely robust in spite of gene flow. We ran both analyses with the reduced dataset (bolded, Table S1) for computational efficiency.

For SNAPP, we sampled backward and forward mutation rates *u* and *v* with initial values = 1 and sampled the speciation rate λ within *T. sirtalis* under an improper prior distribution (1/*x*). For the population size parameter, we applied a gamma distribution prior with a mean $\alpha/\beta = 0.0085$, which represents the mean number of variants/site found in the total dataset used for the population structure analysis and the reduced set used for species tree estimation. We ran two replicate analyses with a random starting seed for 5,000,000 steps, sampling every 100 and then removed the first 25% as burn-in. We checked for stability in posterior estimates and log likelihood of the results of the combined runs in Tracer 1.7 (Rambaut et al., 2018) and visualized the results in DensiTree (Bouckaert, 2010).

For BPP, we estimated a species tree ('A01' analysis) from all loci under a Jukes-Cantor substitution model and set inverse gamma priors (α, β) for the root divergence prior tau (4, 0.001) and population size prior theta (4, 0.002). We ran two replicate analyses for 100,000 generations, sampling every two iterations. We discarded the first 30,000 iterations as burn-in and combined the results of the independent runs to increase sampling from the posterior.

2.7 | Demographic analyses

Divergence time estimation in coalescent species tree analyses can be confounded by migration, population size changes through time and population structure (Barley et al., 2018; Stange et al., 2018). We therefore estimated divergence times and additional demographic patterns from the reduced dataset in momi2 (Kamm et al., 2020), which fits the observed site frequency spectrum to that expected under a continuous-time Moran model (Durrett, 2002). We evaluated the fit of 18 models (Table S3) representing historic population size changes and varying degrees of secondary contact between lineages that might reflect late Miocene–Pleistocene range contractions and expansions. We allowed population sizes and divergence times to vary with starting values picked using a random seed, and we optimized each model over five runs under the 'L-BFGS-B' algorithm, with a maximum of 100 iterations. Here, Model 0 is a null model simply reflecting the consensus species tree topology inferred from SNAPP and BPP with no demographic events (i.e. divergence with no population size change or gene flow, similar in approach to Corbett et al., 2020). Each subsequent model includes an additional demographic parameter (migration time, probability of migration, population size change), with Model 17 being the most complex (a species tree

with estimates for migration time and probability for each lineage pair as well as lineage-specific population size change estimates). We assumed a generation time of 3 years and a mutation rate of 2.43×10^{-9} per site per generation, as recently estimated from the *T. sirtalis* genome (Perry et al., 2018). We ranked the models using Akaike information criterion (AIC) scores (Akaike, 1973).

2.8 | Species distribution modelling

We constructed species distribution models (SDMs) for *T. sirtalis* using `MAXENT` (Phillips et al., 2006) implemented in `ENMTools` (Warren et al., 2010). We generated 'lineage ranges' from polygons constructed from the outermost coordinates of the samples used in the genetic analyses and the coordinates within for unique and spatially rarefied georeferenced research grade *T. sirtalis* occurrences ($n = 9776$) from GBIF (GBIF.org, 2019). For environmental data, we stacked rasters for elevation data, 19 bioclimatic variables derived from temperature, seasonality and precipitation records (Fick & Hijmans, 2017), and proximity to water (Lehner et al., 2008). We then deleted variables with a Pearson's correlation coefficient >0.75 to remove multicollinearity, which reduced the dataset to nine bioclimatic variables related to temperature, mean diurnal range, precipitation, elevation, and proximity to water. We withheld 25% of the occurrence points to train the model (Syfert et al., 2013) to minimize overfitting the model to the data (Warren & Seifert, 2011). We ranked model efficacy with the area under the curve (AUC) score, which measures model discrimination accuracy (Phillips et al., 2006). We quantified habitat similarity between *T. sirtalis* lineages with asymmetric background tests. This test calculates Schoener's *D* (Schoener, 1968) and Warren's *I* statistics (Warren et al., 2008) by comparing the environmental similarity of one SDM to that of a distribution of SDMs generated from randomly selected pseudoabsence points from the range of the other, which in the process accounts for environmental heterogeneity within the sampled space. Deviations in habitat similarity from the null distribution of pseudoreplicate SDMs might represent non-random niche differentiation between populations. We ran this background similarity test 100 times for each SDM pair to achieve high statistical resolution (approximate $p = 0.01$) per user manual guidelines.

To characterize habitat suitability changes that putatively led to historic isolation or secondary contact between subpopulations during restriction to shared refugia, we back-projected present-day SDMs onto Pleistocene and Miocene climate data from the PaleoClim database (Brown et al., 2018). We used projections for the mid-Pliocene warm period (3.205 Ma; Hill, 2015), the Middle Pleistocene (787 ky; Brown et al., 2018), the Last Interglacial Period (130 ky; Otto-Bliesner et al., 2006) and the Last Glacial Maximum (LGM, 21 ky; Karger et al., 2021). Not all bioclimatic variables are represented in these projections, so we generated SDMs with a subset of variables represented in palaeoclimate datasets (bio1, bio4, bio12, bio14, bio15 and bio18) using the same approach as the present-day models and predicted habitat suitability with the *predict* function in `DISMO` (Hijmans et al., 2017).

3 | RESULTS

3.1 | Genomic data

The thamnophiine *cytB* alignment consisted of 812 bp from 99 individuals, with 530 identical sites. `stacks` processed 19,065 loci (865,438 sites) consisting of 10,896 SNPs across 195 samples. For all samples, an average of 65% of the total reads were retained. The `IQ-TREE2` reduced dataset contained 9741 autosomal loci with 8321 SNPs and 719 Z-linked loci with 567 SNPs. The reduced four sample/population assembly for the species tree and demographic analyses consisted of 9023 loci with 4288 unlinked SNPs, with no missing data.

3.2 | Population structure

Principal components analysis and `TESS3r` analyses of the complete dataset (Figure 2) identified four geographical clusters corresponding to the West Coast and Pacific Northwest (the 'west' cluster), the extent of the Mississippi Watershed and along the Rio Grande in the southwestern United States ('central'), the mid-Atlantic coast and the northeastern extent of the Appalachian Highlands ('east') and the southeast Atlantic Coastal Plain ('southeast'). The average majority ancestry coefficient values were similar across the inferred populations, with the central population being the most admixed (average 'central' ancestry coefficient = 0.74, SD = 0.12, $n = 51$), and the southeast the least admixed (0.82, SD = 0.19, $n = 30$). In the PCAs of all three SNP datasets, PC1 explained variance along a longitudinal gradient, with PC2 differentiating the southeast cluster from all others. The amount of variance captured by PC1 and PC2 was substantially higher in analyses of the total and autosomal datasets than the Z-linked dataset, in part due to the lower number of Z-linked SNPs captured. Population differentiation from pairwise F_{ST} estimates (Table 1) increased with space, with southeast and west populations being the most differentiated ($F_{ST} = 0.163$) and the adjacent central and east populations being the least ($F_{ST} = 0.049$). Overall heterozygosity and nucleotide diversity in all populations was lower in the Z chromosome. Most measures of genetic diversity (Table 2) were similar across the different rangewide datasets, with F_{ST} values being higher in the reduced and Z-linked datasets due to lower sample size and lower N_e respectively. Among populations, the west population exhibited the highest inbreeding coefficient ($F_{IS} = 0.391$) and the west and southeast showed slightly higher total genetic diversity (H_T for the west = 0.136 and for the southeast = 0.131), than the central and east (H_T for the central = 0.094 and for the east = 0.085).

Principal components analysis analyses of the three datasets consistently partitioned variation between the southeast and remaining populations (Figure 2; Figure S1). However, structure between the central, east and west populations differed between datasets, with Z-linked loci exhibiting less differentiation between the west and central populations, and autosomal loci clustering the east and central populations. Our `EEMS` results (Figure 2) showed

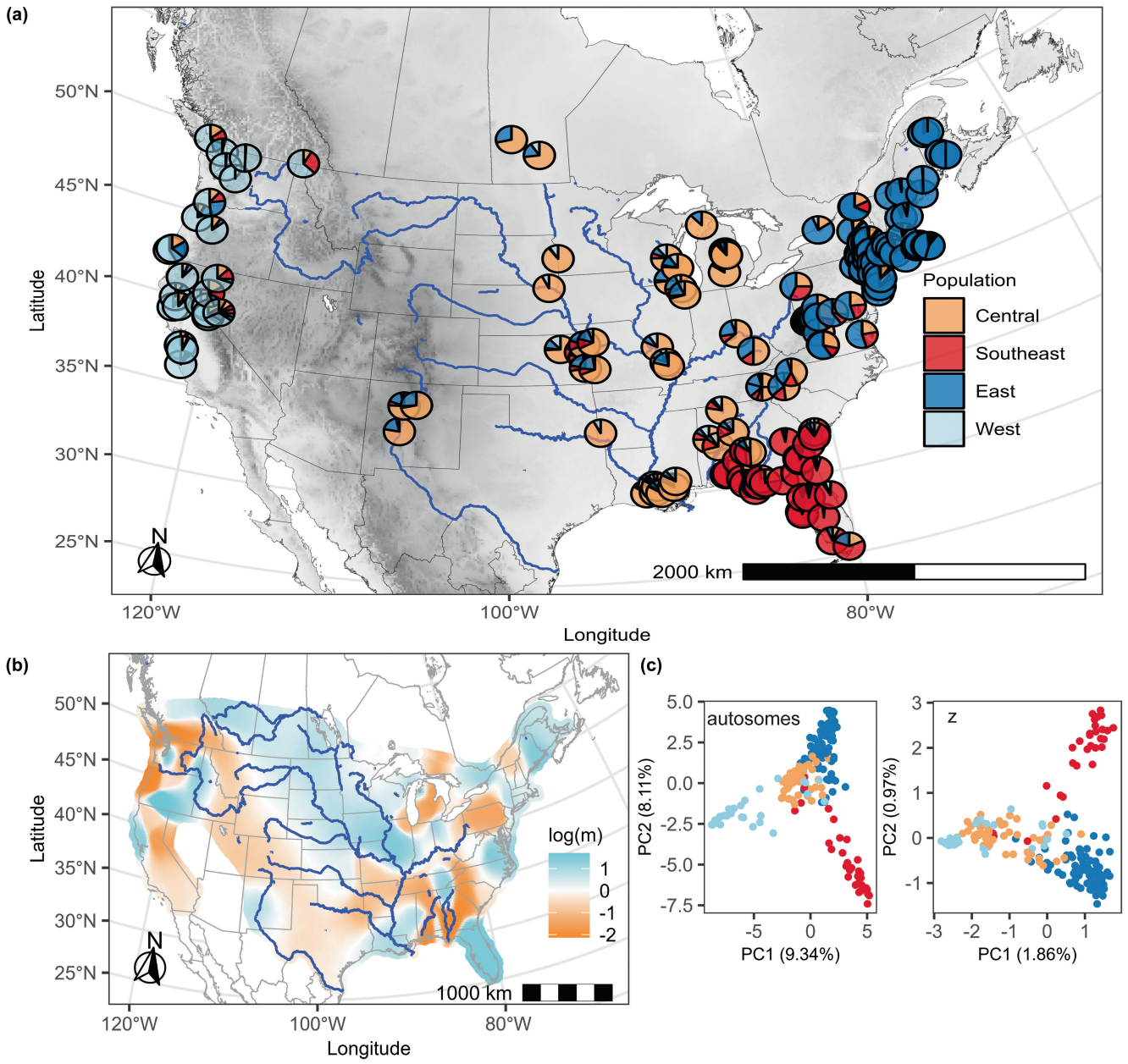

FIGURE 2 Population genetic structure results within *Thamnophis sirtalis*. (a) `TESS3r` results support a $K=4$ model, with populations conforming to the limits of the Mississippi Watershed ("central" population), the southeast Atlantic Coastal Plain (the 'southeast' population), the Pacific Coast and Pacific Northwest ('west') and the Appalachian Highlands and Atlantic Coast ('east'). (b) `EEMS` results suggest depressed gene flow flanking the regions around the Apalachicola-Chattahoochee-Flint River Basin and major mountain systems in the east and west extents of *T. sirtalis*' range. (c) Principal components analysis results of chromosomal datasets exhibit congruence in population differentiation between the southeast and all other populations, with results from Z-linked single nucleotide polymorphisms (bottom) exhibiting a pattern of genetic similarity between the central and west populations.

low migration rates across the southeast Atlantic Coastal Plain, with latitudinal barriers corresponding to the ACF River basin and the Alabama River. Similarly, inferred low migration rates in the west subtended the Columbia Basin between the Rocky and Cascade Mountain systems in the Pacific Northwest and demarcated the uninhabited desert southwest along the border of western California. In the northeast, migration barriers between the central and eastern populations corresponded to the Appalachian Highlands.

3.3 | Phylogenetic relationships

The mtDNA tree topology showed similar relationships and divergence time estimates for *Thamnophis* as prior studies (Alfaro & Arnold, 2001; De Queiroz et al., 2002; Hallas et al., 2022; McVay et al., 2015; Nuñez et al., 2023). *T. sirtalis* clades represented geographically structured lineages congruent with those inferred by SNP-based population structure analyses (Figure 3). Fossil calibrated divergence time estimates

from *cytB* supported a late Miocene/early Pliocene divergence (6.3 Mya, 95% highest posterior density: 3.9–8.9) between the southeast clade restricted to the Atlantic Coastal Plain and the rest of the tree. The east lineage occupies the northeast extent of the Eastern Forest and extends westward to the eastern edge of the Mississippi Watershed. The remaining individuals formed a strongly supported clade consisting of two weakly supported subclades: the central lineage containing individuals dispersed throughout the Mississippi Watershed west of the Ohio River and those restricted to the Rio Grande, and the west lineage of individuals found east of the Interior Plains.

Both the autosomal and Z-linked SNP trees (Figure 3) supported the monophyly of the southeast lineage to the exclusion of one southeast individual from southern Alabama (located west of the ACF River Basin) nested within the central clade. The western lineage was similarly monophyletic for both autosomal and Z-linked trees with the exception of an inland California individual from east of the Sierra Nevada Mountains.

The SNAPP and BPP topologies (Figure S2) mostly agreed with mtDNA clade relationships. Both analyses supported the initial divergence event separating the southeast lineage from the rest, but moderately supported the east/central + west divergence (posterior probability (PP) = 0.88 for SNAPP, PP = 0.92 for BPP). While the tree topologies with the highest posterior probabilities inferred by BPP all exhibited strong support for the placement of the southeast group, visualization of the SNAPP analyses by DensiTree showed some ambiguity in the relationship between the southeast and east groups.

TABLE 1 Mean pairwise F_{ST} values for population pairs of *Thamnophis sirtalis* across datasets calculated in hierfstat.

Population pair	Total	Reduced	Z	Autosomes
East–Central	0.049	0.151	0.162	0.045
East–Southeast	0.117	0.253	0.152	0.110
East–West	0.121	0.341	0.241	0.123
Central–Southeast	0.107	0.279	0.165	0.106
Central–West	0.072	0.216	0.104	0.077
Southeast–West	0.163	0.443	0.240	0.169

3.4 | Divergence times and demographic analysis

Thirteen of 18 tested models reached convergence during optimization (Table S3). The AIC results for converged analyses support the highest ranked model with a wAIC score of 1.0 (Figure 4, Model 16 in Table S3). This model supported a middle Pleistocene (~1 Mya) divergence between the southeast and all other populations with similarly timed Late Pleistocene population changes in the remaining lineages (additional model tests and parameter estimates in Table S3). The divergence between the east and central/west lineages occurred at ~750 kya, followed by the central/west 500 kya, substantially younger splits than those inferred from the fossil-calibrated mtDNA tree. The east and central contemporary population sizes were similarly sized (N_{East} = 233,893, $N_{central}$ = 204,990) and larger than the southeast ($N_{Southeast}$ = 124,843) and west (N_{West} = 56,163) estimates. We note that $N_{Southeast}$ was nearly 3× greater than N_{West} despite the difference in overall range size. Only the east lineage exhibited a population size increase, with a recovery from a historic bottleneck timed at 167 kya. The central and west lineages exhibited bottlenecks timed at ~121 and ~262 kya respectively. However, the population size change was markedly more extreme in the central lineage, with a higher than 10-fold decrease from a high ancestral population size of over 2,154,522 individuals compared to the 1.5× decrease observed in the west. Population size change in the southeast population was not estimated in the top ranked model. Inferred pulse probabilities (PP*, migration events) were relatively low between lineages with the highest representing central migration into the southeast (PP* = 0.27) and east (PP* = 0.21) in the Late Pleistocene.

TABLE 2 Data characteristics and population summary statistics calculated in hierfstat: observed per-locus heterozygosity (H_O), within population genetic diversity (H_S), total genetic diversity (H_T) and coefficient of inbreeding (F_{IS}).

Dataset	# Individuals	# Loci	# Variants	H_O	H_S	H_T	F_{IS}
Total	195	19,065	10,896	0.045	0.065	0.071	0.301
Autosomes	195	9743	9042	0.046	0.065	0.071	0.283
Z chromosome	195	719	651	0.038	0.060	0.071	0.361
IQ-TREE2 (Z)	59	719	567	0.079	0.116	0.141	0.316
IQ-TREE2 (autosomes)	59	9741	8321	0.086	0.113	0.113	0.240
Reduced	16	9023	4288	0.087	0.120	0.156	0.274
West	29	13,330	6173	0.083	0.136	0.136	0.391
Central	51	16,530	8699	0.073	0.094	0.094	0.225
Southeast	30	15,509	8238	0.103	0.131	0.131	0.212
East	85	17,028	9512	0.063	0.085	0.085	0.262

Note: Additional raw and corrected summary statistics are available in Table S4.

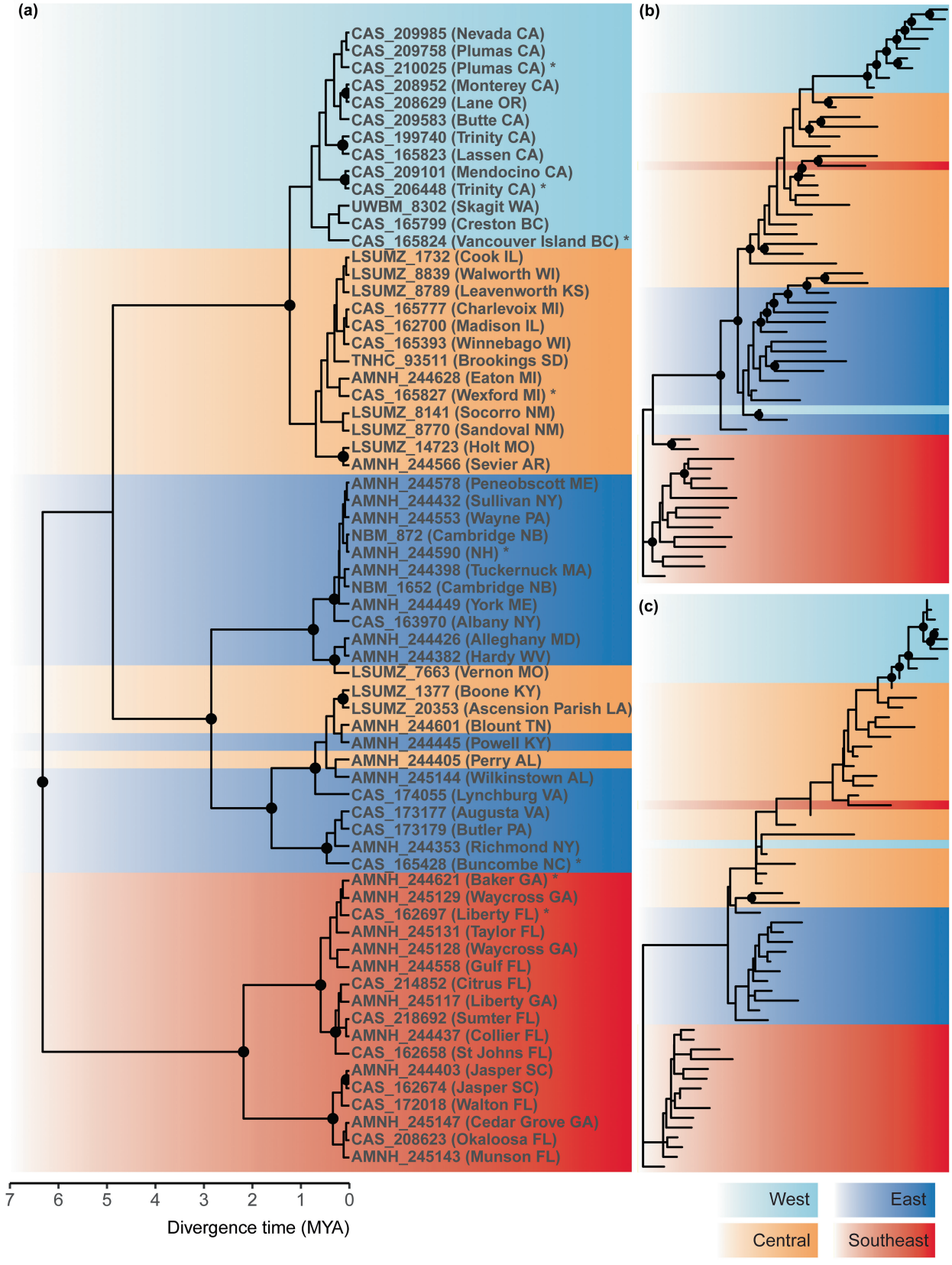

FIGURE 3 Phylogenetic relationships within *Thamnophis sirtalis*. (a) *cytB* maximum clade credibility tree estimated in BEAST 1.10. (b) Autosomal-derived and (c) Z-linked SNP trees estimated in IQ-TREE2. Nodes with black dots have posterior probabilities >0.90. Asterisked samples in the *cytB* tree are not represented in the SNP-based analyses. The thamnophiine and IQ-TREE2 treefiles are available in the Supporting Information. SNP, single nucleotide polymorphism.

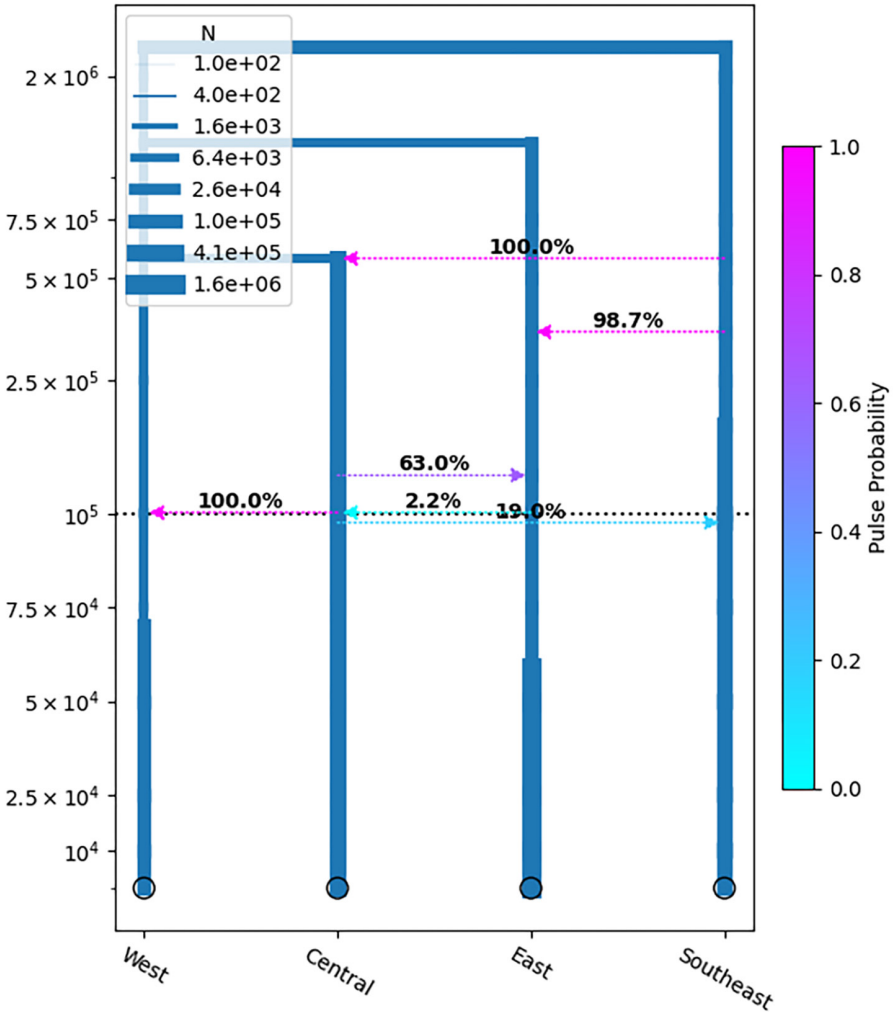

FIGURE 4 The highest ranked demographic model from `momi2` by Akaike informaiton criterion. The left axis represents time in years, and blue arrows between lineages indicate probability of directional gene flow between lineages (e.g. the 'pulse probability' between the southeast and east lineages is much higher than between the southeast and central). Branch width reflects population size (denoted in the inset by *N*). The highest ranked model supports an early Pleistocene divergence (~2.4 Mya) between the southeast and remaining *Thamnophis sirtalis* populations, followed by parallel late Pleistocene size changes in the east (increase, ~150 kya) and central (bottleneck, ~100 kya) lineages.

3.5 | Ecological niche modelling/overlap

All present-day SDMs for the *T. sirtalis* populations (Figure 5) exhibited high AUC values (>0.9). The west population SDM was the most restricted and the only model that represents the modern boundaries, while the remaining models all predicted some degree of habitat suitability in the western extent of *T. sirtalis*, particularly in the coastal Pacific Northwest. The inferred suitable habitat for the present-day central SDM extended into peninsular Florida, while the southeast SDM was mostly restricted to the Gulf Coast. The east population SDM was the least restricted to its realized extent, with suitable habitat inferred in large but fragmented expanses of eastern and western NA as well as the forested regions of the base of the Rocky Mountain system. For the asymmetric background tests (Table 3), niche overlap as a measure of *D* and *I* statistics was higher in comparisons between the adjacent populations occupying eastern NA, with the highest overlap observed in the east-central and southeast-central comparisons. The lowest observed overlap was in the geographically disparate southeast–west comparison.

Back-projection of the present-day SDMs to different historical timepoints back to the Middle Pliocene yielded noticeably different results between populations (Figure S5). The central SDM exhibited the widest suitable habitat breadth at all time periods and shows a general restriction to below the glacial line and north of peninsular southeast during the LGM (~21 kya). This LGM southward contraction was also reflected in the east SDM, while the geographical extents of west and southeast SDMs were consistently restricted throughout the Pleistocene.

4 | DISCUSSION

Within *T. sirtalis* we identify four distinct geographical lineages with distributions in the west, east, southeast and central NA. We show that established vicariant barriers, habitat shifts and Pleistocene glacial history drives lineage formation throughout this distribution. We find support for the broad and fine-scale structuring effects of northern mountain systems as well as the role of multiple basins in both restricting and facilitating expansion. Sex-linked markers show a pattern of genetic similarity between west and central clusters consistent with westward expansion across/over the Interior Plains. Simulations under demographic and historical ecological niche models support a scenario where global climate fluctuations and sea level changes led to geographical restriction to southern refugia and ensuing secondary

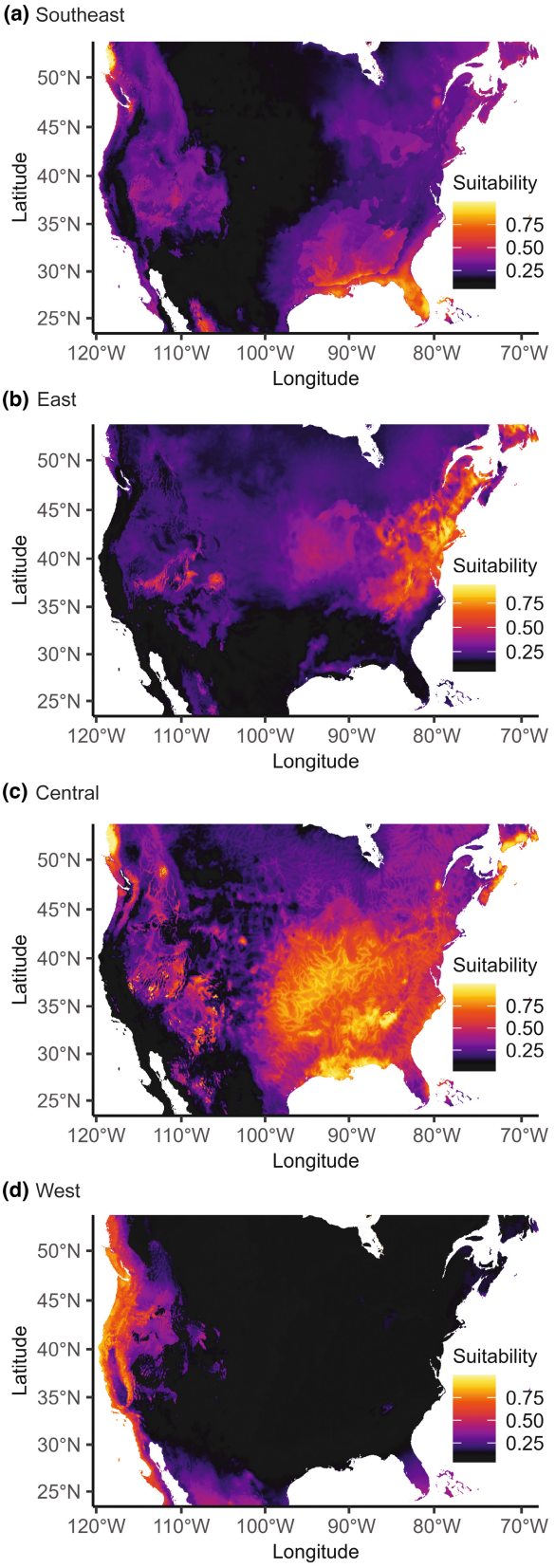

FIGURE 5 Species distribution models (SDMs) for *Thamnophis sirtalis* generated by MAXENT in `ENMTools`. Models were developed using spatially rarified research-grade georeferenced GBIF occurrences ($n = 9776$) within the outer spatial bounds of the southeast (a), east (b), central (c) and west (d) populations inferred from `TESS3r`. Present-day SDMs shown were generated from the complete WorldClim bioclimatic dataset as well as elevation and proximity to water, while back projections represent those of SDMs for the subset of variables represented in all PaleoClim models. Warmer colours indicate probability of habitat suitability.

contact between established eastern lineages, followed by northward expansion following glacial retreat. We find that no lineages explicitly correspond to subspecies boundaries, corroborating prior genetic investigations' conclusions concerning their lack of validity.

4.1 | Phylogeography

The phylogeographic structure of *T. sirtalis* identifies the Atlantic Coastal Plain as the extent of a highly diverged southeast subpopulation and the ACF River Basin and Alabama River as local barriers to gene flow. Similar to patterns found in numerous taxa (Conant & Collins, 1998; Peterson, 1999; Soltis et al., 2006) and snakes in particular (Burbrink et al., 2008; Burbrink, Bernstein, et al., 2021; Burbrink, Gehara, et al., 2021; Burbrink & Guiher, 2015; Fontanella et al., 2008; Myers et al., 2020), the deepest phylogenetic split within *T. sirtalis* is between a clade largely restricted to this region and all other clades, reflecting the shared effects of potential fidelity to the low elevation subtropical climate and the historic glacial cycles that repeatedly isolated the region from the mainland (Webb, 1990). Highly admixed individuals sampled between the ACF River Basin and the Alabama River provide evidence of historic or ongoing gene flow between the southeastern and central populations, but this riverine barrier pattern is absent along the Lower Mississippi River.

The southern boundary of the east population corresponds to where the basins of the Tennessee and Ohio Rivers join the lower boundary of the Appalachian Highlands. Admixture patterns in this region suggest secondary contact between the east, southeast and central populations. We cannot confirm continuous gene flow along the mid-Atlantic Coast here due to sampling gaps. However, taken with slightly lower migration rate estimates in this area compared to those inferred along the ACF and Alabama River systems, it is likely that rivers comprising the eastern portion of the Mississippi Watershed facilitated northeastward expansion following southern isolation during the LGM. Further corroborating this scenario is the extent of overlapping suitable habitat observed in back projection of the present-day SDMs of the east, central and southeast populations (Figure 5; Figure S5). The northernmost sampled individuals of the east population exhibit substantially less admixture as expected from recent founder populations.

The range of the central population extends from the river networks of the Mississippi Watershed into the northern and western extents of the Interior Plains and encompasses a large east–west shift in habitat type from eastern temperate mixed forest to arid prairie grassland. The inferred assignment of the disjunct Rio Grande subpopulation of the southwestern United States to the central population can be explained by previously hypothesized Pleistocene connectivity between the Upper Arkansas River and the head of the

TABLE 3 Empirical asymmetric background test summary statistics (Schoener's *D*, Warren's *I*, Spearman correlation coefficients) for geographical space and environment.

Population comparison	*D*	*I*	Cor	D_{env}	I_{env}	Cor_{env}	*p*-Value
Central–West	0.083	0.260	−0.481	0.080	0.219	−0.391	0.010
East–Central	0.332	0.625	0.465	0.077	0.226	0.087	0.010
East–Southeast	0.076	0.251	0.283	0.130	0.270	0.400	0.010
East–West	0.052	0.156	0.171	0.040	0.109	−0.023	0.010
Southeast–Central	0.276	0.588	0.534	0.125	0.310	0.103	0.010
Southeast–West	0.010	0.066	−0.380	0.037	0.101	−0.016	0.010

Note: For each population comparison, higher *D* and *I* values indicate greater niche overlap and equivalency, respectively, between populations. Histograms comparing the empirical values to the distribution of 100 psuedoreplicates can be found in Figure S2.

Rio Grande at the San Luis Drainage Basin (Repasch et al., 2017; Rogers et al., 1992; Ruleman et al., 2019).

Historic riverine networks in the Upper Missouri sub-basin of the Mississippi Watershed likely facilitated rapid expansion of *T. sirtalis* into the Pacific Northwest via the low elevation passes of the Northern Rocky Mountains in present-day Montana, followed by southward dispersal down the Pacific Coast and east of the Sierra Nevada Mountains. Inferred admixture patterns show differentiation between coastal and inland (east of the Sierra Nevada) *T. sirtalis* populations, but these clusters within California do not exhibit strong phylogeographical structure, likely due in part to both the recency of the founder event and historic and/or ongoing gene flow. Future sampling and sequencing efforts should emphasize the isolated populations of the Northern Rockies and the Interior Plains, which are rare in modern collections and will be crucial in better characterizing westward post-Pleistocene expansion.

4.2 | Population differentiation across space and the genome

We interpret the lower F_{IS} in the west population as a sign of postglacial expansion following significant Pleistocene isolation in western refugia, whereas higher levels of diversity in eastern populations might have been maintained by secondary contact with other populations in shared refugia. The greater differentiation between the northward expanding west and east populations in the Z chromosome warrants further study. In addition to being linked to historic demographic shifts in populations, the Z chromosome has been associated with maintaining diversity in hybridizing species pairs (Battey, 2020), maintaining deviations low heterozygosity in populations under selection (Gendreau et al., 2020), phenotypic differentiation (Sæther et al., 2007; Toews et al., 2016), sex-biased dispersal (Li & Merilä, 2010) and speciation (Qvarnström & Bailey, 2009). Future work with more robust interrogation of the genome can provide greater understanding of genomic and spatial patterns of intraspecific diversification with ongoing gene flow.

4.3 | Divergence timing and demography

Our mtDNA divergence time estimates for a mid-Miocene origin of the clade containing *T. sirtalis*, *T. sauritus* and *T. proximus* are expectedly older than those from recent multilocus studies of the Northern/widespread *Thamnophis* subclade to which it belongs (12.21 Mya, Hallas et al., 2022; 11.97 Mya, Nuñez et al., 2023). These differences reflect known patterns of discordance between single and multilocus approaches (Edwards & Beerli, 2000), which might also be biased by older fossil calibration points in the mtDNA analysis (Arbogast et al., 2002; Zheng et al., 2011). Taken together, we conclude a early Pliocene origin in the central or southeastern NA for *Thamnophis*. This period was characterized by the expansion of North American grasslands and is associated with an increase in snake diversification as evidenced in the fossil record and broader thamnophiine and natricid phylogenetic studies (Guo et al., 2012; Holman, 2000; McVay et al., 2015; Nuñez et al., 2023).

The timing of divergence of the southeast lineage from the other lineages inferred from SNP data and minimal inferred admixture further support a history of periodic isolation due to rising sea levels associated with Pleistocene glacial cycles (Webb, 1990). These processes have been found to affect contemporary population structure in many distantly related species distributed across the east and southeastern United States (Kozak et al., 2005; Soltis et al., 2006). Divergence time estimates for the remaining lineages conclusively point to expansions into western and northeastern NA prior to refugial isolation during the LGM. Supporting conclusions from prior investigations of *T. sirtalis* in western NA and the Great Lakes (Janzen et al., 2002; Placyk et al., 2007), our demographic analyses support recent gene flow (post-LGM) from the central lineage to the west. It also shows historic (pre-LGM) symmetric gene flow between the central and east lineages, supporting a scenario of post-glacial expansion from both southern and northern refugia. The secondary contact between southeast, east and central lineages might explain their high levels of genetic diversity compared to the west where LGM refugia along the Pacific Coast were isolated from other lineages.

4.4 | Ecological diversification

Our ecological niche modelling analyses give context to the demographic history of *T. sirtalis* and provide a clearer picture of spatial changes in habitat suitability through time. The wide fundamental niche of the central population inferred from its present-day SDM extends into the ranges of both east and southeast populations, supporting a scenario of gene flow facilitated by shared habitat between them. Different populations of *T. sirtalis* populations can vary widely in ecology (Rossman et al., 1996), and the predicted niche space of the central population compared to that of the others could be explained by variation in dispersal ability due to unique life-history traits (e.g. fidelity to overwintering den sites, differential responses to aridity). With additional evidence from genetic data and ecological modelling, we find support for Pleistocene genetic structuring due to isolation in refugia distributed throughout intermontane forest and coastal habitat in the west, subtropical marshland in the extreme southeast and the Appalachian foothills and inland coastal plains of the east and southeast.

4.5 | Taxonomy

Analyses of mtDNA and morphological data have already highlighted the invalidity of *T. sirtalis* subspecies as evolutionary units (Boundy, 1999; Janzen et al., 2002; Rossman et al., 1996). The discrete genetic populations identified here do not correspond to morphological subspecies described in prior studies (Figures 1 and 2). Additionally, we provide evidence of recent gene flow where contact zones exist and signatures of historic gene flow between lineages that are currently disconnected. We refrain from proposing any taxonomic revisions until the extent of population boundaries can be clarified with more samples and whole-genome data.

ACKNOWLEDGEMENTS

We thank the Washington Department of Fish and Wildlife for collecting permits issued to LNJ (SCP #14-260) and UW IACUC for approval of live animal protocols to LNJ. The authors dedicate this study to Douglas A. Rossman and Robin Lawson, whose indelible contributions to our understanding of natricid evolution and ecology laid the foundation for this study. Multiple museum institutions contributed tissue samples used in this study. The authors are especially grateful for Sharon Birks and Kevin Epperly (UWBM), Luke Welton (KU), Jens Vindum (CAS), Mary Sollows (NBM), David Kizirian, Margaret Arnold, David Dickey and Lauren Vonnahme (AMNH), Eli Greenbaum (UTEP), Travis LaDuc (TNHC), Donna Dittmann (LSUMZ), Gregory Watkins-Colwell (YPM) for the processing and contribution of catalogued tissue loans used for this study. Joe Felsenstein, Kerry Naish and Richard Olmstead contributed guidance to the development of the study and the Davis-Rabosky lab provided comments that greatly improved the manuscript. This work was supported by grants from the National Science Foundation (DEB #1600844) and the American Museum of Natural History (Theodore Roosevelt Award) awarded to LNJ.

CONFLICT OF INTEREST STATEMENT

The authors declare no conflict of interest.

DATA AVAILABILITY STATEMENT

Demultiplexed ddRADseq data, mtDNA alignments, input files, and scripts for analyses and figure generation are hosted on DRYAD (https://doi.org/10.5061/dryad.280gb5mtm).

ORCID

Leonard N. Jones II https://orcid.org/0000-0002-2548-8546
Adam D. Leaché https://orcid.org/0000-0001-8929-6300
Frank T. Burbrink https://orcid.org/0000-0001-6687-8332

REFERENCES

Akaike, H. (1973). Maximum likelihood identification of Gaussian autoregressive moving average models. *Biometrika*, *60*(2), 255–265. https://doi.org/10.1093/biomet/60.2.255

Alfaro, M. E., & Arnold, S. J. (2001). Molecular systematics and evolution of regina and the thamnophiine snakes. *Molecular Phylogenetics and Evolution*, *21*(3), 408–423. https://doi.org/10.1006/mpev.2001.1024

Allen, L. S. (2005). *Phylogeography of five subspecies of western ribbon snakes (Thamnophis proximus) in the United States and Middle America*. The University of Texas at Arlington.

Arbogast, B. S., Edwards, S. V., Wakeley, J., Beerli, P., & Slowinski, J. B. (2002). Estimating divergence times from molecular data on phylogenetic and population genetic timescales. *Annual Review of Ecology and Systematics*, *33*(1), 707–740. https://doi.org/10.1146/annurev.ecolsys.33.010802.150500

Austin, J. D., Lougheed, S. C., & Boag, P. T. (2004). Discordant temporal and geographic patterns in maternal lineages of eastern North American frogs, *Rana catesbeiana* (Ranidae) and *Pseudacris crucifer* (Hylidae). *Molecular Phylogenetics and Evolution*, *32*(3), 799–816. https://doi.org/10.1016/j.ympev.2004.03.006

Avise, J. C. (2000). *Phylogeography: The history and formation of species*. Harvard University Press.

Bailey, R. G. (1995). *Description of the ecoregions of the United States*. U.S. Department of Agriculture, Forest Service.

Baker, R. J., Mengden, G. A., & Bull, J. J. (1972). Karyotypic studies of thirty-eight species of North American snakes. *Copeia*, *1972*(2), 257. https://doi.org/10.2307/1442486

Barley, A. J., Brown, J. M., & Thomson, R. C. (2018). Impact of model violations on the inference of species boundaries under the multispecies coalescent. *Systematic Biology*, *67*(2), 269–284. https://doi.org/10.1093/sysbio/syx073

Battey, C. J. (2020). Evidence of linked selection on the Z chromosome of hybridizing hummingbirds. *Evolution*, *74*(4), 725–739. https://doi.org/10.1111/evo.13888

Beheregaray, L. B. (2008). Twenty years of phylogeography: The state of the field and the challenges for the southern hemisphere. *Molecular Ecology*, *17*(17), 3754–3774. https://doi.org/10.1111/j.1365-294X.2008.03857.x

Bouckaert, R., Heled, J., Kühnert, D., Vaughan, T., Chieh-Hsi, W., Xie, D., Suchard, M. A., Rambaut, A., & Drummond, A. J. (2014). BEAST 2: A software platform for Bayesian evolutionary analysis. *PLoS Computational Biology*, *10*(4), e1003537. https://doi.org/10.1371/journal.pcbi.1003537

Bouckaert, R. R. (2010). DensiTree: Making sense of sets of phylogenetic trees. *Bioinformatics*, *26*(10), 1372–1373. https://doi.org/10.1093/bioinformatics/btq110

Boundy, J. J. (1999). *Systematics of the common garter snake, Thamnophis sirtalis* (Ph.D. thesis). Louisiana State University and Agricultural & Mechanical College, United States, Louisiana.

Bradburd, G. S., Ralph, P. L., & Coop, G. M. (2013). Disentangling the effects of geographic and ecological isolation on genetic differentiation. *Evolution*, *67*(11), 3258–3273. https://doi.org/10.1111/evo.12193

Brodie, E. D. (1968). Investigations on the skin toxin of the adult rough-skinned newt, *Taricha granulosa*. *Copeia*, *1968*(2), 307–313. https://doi.org/10.2307/1441757

Brown, J. L., Hill, D. J., Dolan, A. M., Carnaval, A. C., & Haywood, A. M. (2018). PaleoClim, high spatial resolution paleoclimate surfaces for global land areas. *Scientific Data*, *5*(1), 180254. https://doi.org/10.1038/sdata.2018.254

Brunsfeld, S. J., Sullivan, J., Soltis, D. E., & Soltis, P. S. (2001). Comparative phylogeography of northwestern North America: A synthesis. *Special Publication-British Ecological Society*, *14*, 319–340.

Bryant, D., Bouckaert, R., Felsenstein, J., Rosenberg, N. A., & RoyChoudhury, A. (2012). Inferring species trees directly from biallelic genetic markers: Bypassing gene trees in a full coalescent analysis. *Molecular Biology and Evolution*, *29*(8), 1917–1932. https://doi.org/10.1093/molbev/mss086

Buckley, L. B., & Jetz, W. (2007). Environmental and historical constraints on global patterns of amphibian richness. *Proceedings of the Royal Society B: Biological Sciences*, *274*(1614), 1167–1173. https://doi.org/10.1098/rspb.2006.0436

Burbrink, F. T. (2002). Phylogeographic analysis of the cornsnake (*Elaphe guttata*) complex as inferred from maximum likelihood and Bayesian analyses. *Molecular Phylogenetics and Evolution*, *25*(3), 465–476. https://doi.org/10.1016/S1055-7903(02)00306-8

Burbrink, F. T., Bernstein, J. M., Kuhn, A., Gehara, M., & Ruane, S. (2021). Ecological divergence and the history of gene flow in the Nearctic milksnakes (*Lampropeltis triangulum* complex). *Systematic Biology*, *71*, 839–858. https://doi.org/10.1093/sysbio/syab093

Burbrink, F. T., Chan, Y. L., Myers, E. A., Ruane, S., Smith, B. T., & Hickerson, M. J. (2016). Asynchronous demographic responses to Pleistocene climate change in eastern Nearctic vertebrates. *Ecology Letters*, *19*(12), 1457–1467.

Burbrink, F. T., Frank Fontanella, R., Pyron, A., Guiher, T. J., & Jimenez, C. (2008). Phylogeography across a continent: The evolutionary and demographic history of the North American racer (Serpentes: Colubridae: *Coluber constrictor*). *Molecular Phylogenetics and Evolution*, *47*(1), 274–288. https://doi.org/10.1016/j.ympev.2007.10.020

Burbrink, F. T., Gehara, M., McKelvy, A. D., & Myers, E. A. (2021). Resolving spatial complexities of hybridization in the context of the gray zone of speciation in North American ratsnakes (*Pantherophis obsoletus* complex). *Evolution*, *75*(2), 260–277. https://doi.org/10.1111/evo.14141

Burbrink, F. T., & Guiher, T. J. (2015). Considering gene flow when using coalescent methods to delimit lineages of North American pitvipers of the genus *Agkistrodon*. *Zoological Journal of the Linnean Society*, *173*(2), 505–526. https://doi.org/10.1111/zoj.12211

Burbrink, F. T., Lawson, R., & Slowinski, J. B. (2000). Mitochondrial DNA phylogeography of the polytypic North American rat snake (*Elaphe obsoleta*): A critique of the subspecies concept. *Evolution*, *54*(6), 12.

Calsbeek, R., Thompson, J. N., & Richardson, J. E. (2003). Patterns of molecular evolution and diversification in a biodiversity hotspot: The California Floristic Province. *Molecular Ecology*, *12*(4), 1021–1029. https://doi.org/10.1046/j.1365-294X.2003.01794.x

Caye, K., Deist, T. M., Martins, H., Michel, O., & François, O. (2016). TESS3: Fast inference of spatial population structure and genome scans for selection. *Molecular Ecology Resources*, *16*(2), 540–548. https://doi.org/10.1111/1755-0998.12471

Caye, K., Jay, F., Michel, O., & François, O. (2018). Fast inference of individual admixture coefficients using geographic data. *The Annals of Applied Statistics*, *12*(1), 586–608. https://doi.org/10.1214/17-AOAS1106

Chardon, N. I., Pironon, S., Peterson, M. L., & Doak, D. F. (2020). Incorporating intraspecific variation into species distribution models improves distribution predictions, but cannot predict species traits for a wide-spread plant species. *Ecography*, *43*(1), 60–74. https://doi.org/10.1111/ecog.04630

Conant, R., & Collins, J. T. (1998). *A field guide to reptiles & amphibians*. Houghton Mifflin Harcourt.

Corbett, E. C., Bravo, G. A., Schunck, F., Naka, L. N., Silveira, L. F., & Edwards, S. V. (2020). Evidence for the Pleistocene arc hypothesis from genome-wide SNPs in a Neotropical dry forest specialist, the rufous-fronted thornbird (Furnariidae: *Phacellodomus rufifrons*). *Molecular Ecology*, *29*(22), 4457–4472. https://doi.org/10.1111/mec.15640

Darriba, D., Taboada, G. L., Doallo, R., & Posada, D. (2012). JModelTest 2: More models, new heuristics and parallel computing. *Nature Methods*, *9*(8), 772.

De Queiroz, A., & Lawson, R. (1994). Phylogenetic relationships of the garter snakes based on DNA sequence and allozyme variation. *Biological Journal of the Linnean Society*, *53*(3), 209–229. https://doi.org/10.1111/j.1095-8312.1994.tb01010.x

De Queiroz, A., & Lawson, R. (2008). A peninsula as an Island: Multiple forms of evidence for overwater colonization of Baja California by the gartersnake *Thamnophis validus*. *Biological Journal of the Linnean Society*, *95*(2), 409–424. https://doi.org/10.1111/j.1095-8312.2008.01049.x

De Queiroz, A., Lawson, R., & Lemos-Espinal, J. A. (2002). Phylogenetic relationships of North American garter snakes (*Thamnophis*) based on four mitochondrial genes: How much DNA sequence is enough? *Molecular Phylogenetics and Evolution*, *22*(2), 315–329. https://doi.org/10.1006/mpev.2001.1074

Deutsch, C. A., Tewksbury, J. J., Huey, R. B., Sheldon, K. S., Ghalambor, C. K., Haak, D. C., & Martin, P. R. (2008). Impacts of climate warming on terrestrial ectotherms across latitude. *Proceedings of the National Academy of Sciences of the United States of America*, *105*(18), 6668–6672. https://doi.org/10.1073/pnas.0709472105

Durrett, R. (2002). *Probability models for DNA sequence evolution*. Springer New York.

Edwards, S. V., & Beerli, P. (2000). Perspective: Gene divergence, population divergence, and the variance in coalescence time in phylogeographic studies. *Evolution: International Journal of Organic Evolution*, *54*(6), 1839–1854. https://doi.org/10.1111/j.0014-3820.2000.tb01231.x

Edwards, S. V., Sally Potter, C., Schmitt, J., Bragg, J. G., & Moritz, C. (2016). Reticulation, divergence, and the phylogeography-phylogenetics continuum. *Proceedings of the National Academy of Sciences of the United States of America*, *113*(29), 8025–8032. https://doi.org/10.1073/pnas.1601066113

Feldman, C. R., Brodie, E. D., Brodie, E. D., & Pfrender, M. E. (2010). Genetic architecture of a feeding adaptation: Garter snake (*Thamnophis*) resistance to tetrodotoxin bearing prey. *Proceedings of the Royal Society B: Biological Sciences*, *277*(1698), 3317–3325. https://doi.org/10.1098/rspb.2010.0748

Fick, S. E., & Hijmans, R. J. (2017). WorldClim 2: New 1-km spatial resolution climate surfaces for global land areas. *International Journal of Climatology*, *37*(12), 4302–4315. https://doi.org/10.1002/joc.5086

Finger, N., Farleigh, K., Bracken, J. T., Leaché, A. D., François, O., Yang, Z., Flouri, T., Charran, T., Jezkova, T., Williams, D. A., & Blair, C. (2022). Genome-scale data reveal deep lineage divergence and a complex demographic history in the Texas horned lizard (*Phrynosoma cornutum*) throughout the Southwestern and Central United States. *Genome Biology and Evolution*, *14*(1), evab260. https://doi.org/10.1093/gbe/evab260

Fitzpatrick, B. M., Placyk, J. S., Jr., Niemiller, M. L., Casper, G. S., & Burghardt, G. M. (2008). Distinctiveness in the face of gene flow: Hybridization between specialist and generalist gartersnakes. *Molecular Ecology*, *17*(18), 4107–4117. https://doi.org/10.1111/j.1365-294X.2008.03885.x

Flouri, T., Jiao, X., Rannala, B., & Yang, Z. (2019). A Bayesian implementation of the multispecies coalescent model with introgression for phylogenomic analysis. *Molecular Biology and Evolution*, *37*, 1211–1223. https://doi.org/10.1093/molbev/msz296

Fontanella, F. M., Feldman, C. R., Siddall, M. E., & Burbrink, F. T. (2008). Phylogeography of *Diadophis punctatus*: Extensive lineage diversity and repeated patterns of historical demography in a transcontinental snake. *Molecular Phylogenetics and Evolution*, *46*(3), 1049–1070. https://doi.org/10.1016/j.ympev.2007.10.017

Fujita, M. K., Leaché, A. D., Burbrink, F. T., McGuire, J. A., & Moritz, C. (2012). Coalescent-based species delimitation in an integrative taxonomy. *Trends in Ecology & Evolution*, *27*(9), 480–488. https://doi.org/10.1016/j.tree.2012.04.012

Garland, T. (1988). Genetic basis of activity metabolism. I. Inheritance of speed, stamina, and antipredator displays in the garter snake *Thamnophis sirtalis*. *Evolution*, *42*(2), 335–350. https://doi.org/10.1111/j.1558-5646.1988.tb04137.x

GBIF.org. (2019). GBIF occurrence download. https://www.gbif.org/occurrence/download/0032071-190918142434337

Gendreau, K. L., Hague, M. T. J., Feldman, C. R., Brodie, E. D., Brodie, E. D., & McGlothlin, J. W. (2020). Sex linkage of the skeletal muscle sodium channel gene (SCN4A) explains apparent deviations from Hardy–Weinberg equilibrium of tetrodotoxin-resistance alleles in garter snakes (*Thamnophis sirtalis*). *Heredity*, *124*(5), 647–657. https://doi.org/10.1038/s41437-020-0300-5

Goudet, J. (2005). Hierfstat, a package for r to compute and test hierarchical F-statistics. *Molecular Ecology Notes*, *5*(1), 184–186. https://doi.org/10.1111/j.1471-8286.2004.00828.x

Gregory, P. T. (1984). Habitat, diet, and composition of assemblages of garter snakes (*Thamnophis*) at eight sites on Vancouver Island. *Canadian Journal of Zoology*, *62*(10), 2013–2022. https://doi.org/10.1139/z84-295

Guo, P., Liu, Q., Yan, X., Jiang, K., Hou, M., Li Ding, R., Pyron, A., & Burbrink, F. T. (2012). Out of Asia: Natricine snakes support the Cenozoic Beringian dispersal hypothesis. *Molecular Phylogenetics and Evolution*, *63*(3), 825–833. https://doi.org/10.1016/j.ympev.2012.02.021

Hague, M. T. J., Feldman, C. R., Brodie, E. D., Jr., & Brodie, E. D., III. (2017). Convergent adaptation to dangerous prey proceeds through the same first-step mutation in the garter snake *Thamnophis sirtalis*. *Evolution*, *71*(6), 1504–1518. https://doi.org/10.1111/evo.13244

Hague, M. T. J., Stokes, A. N., Feldman, C. R., Brodie, E. D., Jr., & Brodie, E. D., III. (2020). The geographic mosaic of arms race coevolution is closely matched to prey population structure. *Evolution Letters*, *4*(4), 317–332. https://doi.org/10.1002/evl3.184

Hallas, J. M., Parchman, T. L., & Feldman, C. R. (2021). The influence of history, geography and environment on patterns of diversification in the Western terrestrial garter snake. *Journal of Biogeography*, *48*(9), 2226–2245. https://doi.org/10.1111/jbi.14146

Hallas, J. M., Parchman, T. L., & Feldman, C. R. (2022). Phylogenomic analyses resolve relationships among garter snakes (*Thamnophis*: Natricinae: Colubridae) and elucidate biogeographic history and morphological evolution. *Molecular Phylogenetics and Evolution*, *167*, 107374. https://doi.org/10.1016/j.ympev.2021.107374

Harris, R. B., Alström, P., Ödeen, A., & Leaché, A. D. (2018). Discordance between genomic divergence and phenotypic variation in a rapidly evolving avian genus (*Motacilla*). *Molecular Phylogenetics and Evolution*, *120*, 183–195. https://doi.org/10.1016/j.ympev.2017.11.020

Hewitt, G. (1996). Some genetic consequences of ice ages, and their role in divergence and speciation. *Biological Journal of the Linnean Society*, *58*(3), 247–276. https://doi.org/10.1006/bijl.1996.0035

Hijmans, R. J., Phillips, S., Leathwick, J., & Elith, J. (2017). *Dismo: Species distribution modeling*. R package version 1(4):1–1.

Hill, D. J. (2015). The non-analogue nature of Pliocene temperature gradients. *Earth and Planetary Science Letters*, *425*, 232–241.

Hoang, D. T., Chernomor, O., von Haeseler, A., Minh, B. Q., & Vinh, L. S. (2018). UFBoot2: Improving the ultrafast bootstrap approximation. *Molecular Biology and Evolution*, *35*(2), 518–522. https://doi.org/10.1093/molbev/msx281

Holman, J. A. (2000). *Fossil snakes of North America: Origin, evolution, distribution, paleoecology*. Indiana University Press.

Irwin, D. E. (2002). Phylogeographic breaks without geographic barriers to gene flow. *Evolution*, *56*(12), 2383–2394. https://doi.org/10.1111/j.0014-3820.2002.tb00164.x

Janzen, F. J., Krenz, J. G., Haselkorn, T. S., & Brodie, E. D. (2002). Molecular phylogeography of common garter snakes (*Thamnophis sirtalis*) in western North America: Implications for regional historical forces. *Molecular Ecology*, *11*(9), 1739–1751. https://doi.org/10.1046/j.1365-294X.2002.01571.x

Jombart, T. (2008). Adegenet: A R package for the multivariate analysis of genetic markers. *Bioinformatics*, *24*(11), 1403–1405.

Kalyaanamoorthy, S., Minh, B. Q., Wong, T. K. F., von Haeseler, A., & Jermiin, L. S. (2017). ModelFinder: Fast model selection for accurate phylogenetic estimates. *Nature Methods*, *14*(6), 587–589. https://doi.org/10.1038/nmeth.4285

Kamm, J., Terhorst, J., Durbin, R., & Song, Y. S. (2020). Efficiently inferring the demographic history of many populations with allele count data. *Journal of the American Statistical Association*, *115*(531), 1472–1487. https://doi.org/10.1080/01621459.2019.1635482

Kapfer, J. M., Sloss, B. L., Schuurman, G. W., Paloski, R. A., & Lorch, J. M. (2013). Evidence of hybridization between common gartersnakes (*Thamnophis sirtalis*) and Butler's gartersnakes (*Thamnophis butleri*) in Wisconsin, USA. *Journal of Herpetology*, *47*(3), 400–405.

Karger, D. N., Nobis, M. P., Normand, S., Graham, C. H., & Zimmermann, N. E. (2021). *CHELSA-TraCE21k v1.0. Downscaled transient temperature and precipitation data since the last glacial maximum*. [Preprint]. https://doi.org/10.5194/cp-2021-30

Kozak, K. H., Blaine, R. A., & Larson, A. (2005). Gene lineages and eastern North American Palaeodrainage Basins: Phylogeography and speciation in salamanders of the *Eurycea bislineata* species complex. *Molecular Ecology*, *15*(1), 191–207. https://doi.org/10.1111/j.1365-294X.2005.02757.x

Leaché, A. D., Koo, M. S., Spencer, C. L., Papenfuss, T. J., Fisher, R. N., & McGuire, J. A. (2009). Quantifying ecological, morphological, and genetic variation to delimit species in the coast horned lizard species complex (*Phrynosoma*). *Proceedings of the National Academy of Sciences of the United States of America*, *106*(30), 12418–12423. https://doi.org/10.1073/pnas.0906380106

Leaché, A. D., & Reeder, T. W. (2002). Molecular systematics of the eastern fence lizard (*Sceloporus undulatus*): A comparison of parsimony, likelihood, and Bayesian approaches. *Systematic Biology*, *51*(1), 44–68. https://doi.org/10.1080/106351502753475871

Lee-Yaw, J. A., Irwin, J. T., & Green, D. M. (2008). Postglacial range expansion from northern refugia by the wood frog, *Rana sylvatica*. *Molecular Ecology*, *17*(3), 867–884. https://doi.org/10.1111/j.1365-294X.2007.03611.x

Lehner, B., Verdin, K., & Jarvis, A. (2008). New global hydrography derived from spaceborne elevation data. *EOS, Transactions American Geophysical Union*, *89*(10), 93–94. https://doi.org/10.1029/2008EO100001

Li, M.-H., & Merilä, J. (2010). Sex-specific population structure, natural selection, and linkage disequilibrium in a wild bird population as revealed by genome-wide microsatellite analyses. *BMC Evolutionary Biology*, *10*(1), 66. https://doi.org/10.1186/1471-2148-10-66

Lobeck, A. K. (1948). *Physiographic provinces of North America; physiographic diagram of North America*. Geographical Press, Division of CS Hammond & Company.

Mason, N. A., Fletcher, N. K., Gill, B. A., Chris Funk, W., & Zamudio, K. R. (2020). Coalescent-based species delimitation is sensitive to geographic sampling and isolation by distance. *Systematics and Biodiversity*, *18*(3), 269–280. https://doi.org/10.1080/14772000.2020.1730475

Mason, R. T. (1993). Chemical ecology of the red-sided garter snake, *Thamnophis sirtalis parietalis*. *Brain, Behavior and Evolution*, *41*(3–5), 261–268. https://doi.org/10.1159/000113848

McKelvy, A. D., & Burbrink, F. T. (2017). Ecological divergence in the yellow-bellied kingsnake (*Lampropeltis calligaster*) at two North American biodiversity hotspots. *Molecular Phylogenetics and Evolution*, *106*, 61–72. https://doi.org/10.1016/j.ympev.2016.09.006

McVay, J. D., Flores-Villela, O., & Carstens, B. (2015). Diversification of North American natricine snakes. *Biological Journal of the Linnean Society*, *116*(1), 1–12. https://doi.org/10.1111/bij.12558

Minh, B. Q., Schmidt, H. A., Chernomor, O., Schrempf, D., Woodhams, M. D., von Haeseler, A., & Lanfear, R. (2020). IQ-TREE 2: New models and efficient methods for phylogenetic inference in the genomic era. *Molecular Biology and Evolution*, *37*(5), 1530–1534. https://doi.org/10.1093/molbev/msaa015

Moritz, C., Langham, G., Kearney, M., Krockenberger, A., VanDerWal, J., & Williams, S. (2012). Integrating phylogeography and physiology reveals divergence of thermal traits between central and peripheral lineages of tropical rainforest lizards. *Philosophical Transactions of the Royal Society B: Biological Sciences*, *367*(1596), 1680–1687. https://doi.org/10.1098/rstb.2012.0018

Myers, E. A., McKelvy, A. D., & Burbrink, F. T. (2020). Biogeographic barriers, Pleistocene refugia, and climatic gradients in the Southeastern Nearctic drive diversification in cornsnakes (*Pantherophis Guttatus* complex). *Molecular Ecology*, *29*(4), 797–811. https://doi.org/10.1111/mec.15358

Nuñez, L. P., Gray, L. N., Weisrock, D. W., & Burbrink, F. T. (2023). The phylogenomic and biogeographic history of the gartersnakes, watersnakes, and allies (Natricidae: *Thamnophiini*). *Molecular Phylogenetics and Evolution*, *186*, 107844. https://doi.org/10.1016/j.ympev.2023.107844

Otto-Bliesner, B. L., Marshall, S. J., Overpeck, J. T., Miller, G. H., Hu, A., & CAPE Last Interglacial Project Members. (2006). Simulating Arctic climate warmth and Icefield retreat in the last interglaciation. *Science*, *311*(5768), 1751–1753. https://doi.org/10.1126/science.1120808

Paris, J. R., Stevens, J. R., & Catchen, J. M. (2017). Lost in parameter space: A road map for stacks. *Methods in Ecology and Evolution*, *8*(10), 1360–1373. https://doi.org/10.1111/2041-210X.12775

Perry, B. W., Card, D. C., McGlothlin, J. W., Pasquesi, G. I. M., Adams, R. H., Schield, D. R., Hales, N. R., Corbin, A. B., Demuth, J. P., Hoffmann, F. G., Vandewege, M. W., Schott, R. K., Bhattacharyya, N., Chang, B. S. W., Casewell, N. R., Whiteley, G., Reyes-Velasco, J., Mackessy, S. P., Gamble, T., … Castoe, T. A. (2018). Molecular adaptations for sensing and securing prey and insight into amniote genome diversity from the garter snake genome. *Genome Biology and Evolution*, *10*(8), 2110–2129. https://doi.org/10.1093/gbe/evy157

Peterson, B. K., Weber, J. N., Kay, E. H., Fisher, H. S., & Hoekstra, H. E. (2012). Double digest RADseq: An inexpensive method for de novo SNP discovery and genotyping in model and non-model species. *PLoS One*, *7*(5), e37135. https://doi.org/10.1371/journal.pone.0037135

Peterson, R. T. (1999). *A field guide to the birds: Eastern and central North America*. Houghton Mifflin Harcourt.

Petkova, D., Novembre, J., & Stephens, M. (2016). Visualizing spatial population structure with estimated effective migration surfaces. *Nature Genetics*, *48*(1), 94–100. https://doi.org/10.1038/ng.3464

Phillips, S. J., Anderson, R. P., & Schapire, R. E. (2006). Maximum entropy modeling of species geographic distributions. *Ecological Modelling*, *190*(3), 231–259. https://doi.org/10.1016/j.ecolmodel.2005.03.026

Placyk, J. S., Jr., Burghardt, G. M., Small, R. L., King, R. B., Casper, G. S., & Robinson, J. W. (2007). Post-glacial recolonization of the Great Lakes region by the common gartersnake (*Thamnophis sirtalis*) inferred from mtDNA sequences. *Molecular Phylogenetics and Evolution*, *43*(2), 452–467. https://doi.org/10.1016/j.ympev.2006.10.023

Purcell, S., Neale, B., Todd-Brown, K., Thomas, L., Ferreira, M. A. R., Bender, D., Maller, J., Sklar, P., de Bakker, P. I. W., Daly, M. J., & Sham, P. C. (2007). PLINK: A tool set for whole-genome association and population-based linkage analyses. *The American Journal of Human Genetics*, *81*(3), 559–575. https://doi.org/10.1086/519795

Qvarnström, A., & Bailey, R. I. (2009). Speciation through evolution of sex-linked genes. *Heredity*, *102*(1), 4–15. https://doi.org/10.1038/hdy.2008.93

Ralph Gibson, A., & Bruce Falls, B. (1979). Thermal biology of the common garter snake *Thamnophis sirtalis* (L.). I. Temporal variation, environmental effects and sex differences. *Oecologia*, *43*(1), 79–97.

Rambaut, A., Drummond, A. J., Xie, D., Baele, G., & Suchard, M. A. (2018). Posterior summarization in Bayesian phylogenetics using Tracer 1.7. *Systematic Biology*, *67*(5), 901–904.

Reding, D. M., Bronikowski, A. M., Johnson, W. E., & Clark, W. R. (2012). Pleistocene and ecological effects on continental-scale genetic differentiation in the bobcat (*Lynx rufus*). *Molecular Ecology*, *21*(12), 3078–3093. https://doi.org/10.1111/j.1365-294X.2012.05595.x

Reding, D. M., Castañeda-Rico, S., Shirazi, S., Hofman, C. A., Cancellare, I. A., Lance, S. L., Beringer, J., Clark, W. R., & Maldonado, J. E. (2021). Mitochondrial genomes of the United States distribution of gray fox (*Urocyon cinereoargenteus*) reveal a major phylogeographic break at the Great Plains suture zone. *Frontiers in Ecology and Evolution*, *9*, 666800.

Repasch, M., Karlstrom, K., Heizler, M., & Pecha, M. (2017). Birth and evolution of the Rio Grande fluvial system in the past 8 Ma: Progressive downward integration and the influence of tectonics, volcanism, and climate. *Earth-Science Reviews*, *168*, 113–164. https://doi.org/10.1016/j.earscirev.2017.03.003

Ricketts, T. H., Dinerstein, E., Olson, D. M., Eichbaum, W., Loucks, C. J., Kavanaugh, K., Hedao, P., Hurley, P., DellaSalla, D., Abell, R., Carney, K., & Walters, S. (1999). *Terrestrial ecoregions of North America: A conservation assessment*. Island Press.

Riddle, B. R. (2016). Comparative Phylogeography clarifies the complexity and problems of continental distribution that drove A. R. Wallace to Favor Islands. *Proceedings of the National Academy of Sciences of the United States of America*, *113*(29), 7970–7977. https://doi.org/10.1073/pnas.1601072113

Ridenhour, B. J., Brodie, E. D., Jr., & Brodie, E. D., III. (2007). Patterns of genetic differentiation in *Thamnophis* and *Taricha* from the Pacific Northwest. *Journal of Biogeography*, *34*(4), 724–735. https://doi.org/10.1111/j.1365-2699.2006.01642.x

Rising, J. D. (1983). The Great Plains hybrid zones. In R. F. Johnston (Ed.), *Current ornithology* (pp. 131–157). Springer US.

Rissler, L. J., & Smith, W. H. (2010). Mapping amphibian contact zones and phylogeographical break hotspots across the United States. *Molecular Ecology*, *19*(24), 5404–5416. https://doi.org/10.1111/j.1365-294X.2010.04879.x

Rochette, N. C., Rivera-Colón, A. G., & Catchen, J. M. (2019). Stacks 2: Analytical methods for paired-end sequencing improve RADseq-based population genomics. *Molecular Ecology*, *28*(21), 4737–4754.

Rogers, K. L., Larson, E. E., Smith, G., Katzman, D., Smith, G. R., Cerling, T., Wang, Y., Baker, R. G., Lohmann, K. C., Repenning, C. A., Patterson, P., & Mackie, G. (1992). Pliocene and Pleistocene geologic and climatic evolution in the San Luis Valley of South-Central Colorado. *Palaeogeography, Palaeoclimatology, Palaeoecology*, *94*(1–4), 55–86. https://doi.org/10.1016/0031-0182(92)90113-J

Rolland, J., Silvestro, D., Schluter, D., Guisan, A., Broennimann, O., & Salamin, N. (2018). The impact of endothermy on the climatic niche evolution and the distribution of vertebrate diversity. *Nature Ecology & Evolution*, *2*(3), 459–464. https://doi.org/10.1038/s41559-017-0451-9

Rossman, D. A., Ford, N. B., & Seigel, R. A. (1996). *The garter snakes: Evolution and ecology*. University of Oklahoma Press.

Ruleman, C. A., Hudson, A. M., Thompson, R. A., Miggins, D. P., Paces, J. B., & Goehring, B. M. (2019). Middle Pleistocene formation of the Rio Grande Gorge, San Luis Valley, South-Central Colorado and North-Central New Mexico, USA: Process, timing, and downstream

implications. *Quaternary Science Reviews*, *223*, 105846. https://doi.org/10.1016/j.quascirev.2019.07.028

Sæther, S. A., Sætre, G.-P., Borge, T., Wiley, C., Svedin, N., Andersson, G., Veen, T., Haavie, J., Servedio, M. R., Bureš, S., Král, M., Hjernquist, M. B., Gustafsson, L., Träff, J., & Qvarnström, A. (2007). Sex chromosome-linked species recognition and evolution of reproductive isolation in flycatchers. *Science*, *318*(5847), 95–97. https://doi.org/10.1126/science.1141506

Schoener, T. W. (1968). The *Anolis* lizards of Bimini: Resource partitioning in a complex fauna. *Ecology*, *49*(4), 704–726. https://doi.org/10.2307/1935534

Shafer, A. B. A., Cullingham, C. I., Côté, S. D., & Coltman, D. W. (2010). Of glaciers and refugia: A decade of study sheds new light on the phylogeography of Northwestern North America. *Molecular Ecology*, *19*(21), 4589–4621. https://doi.org/10.1111/j.1365-294X.2010.04828.x

Shine, R., Elphick, M. J., Harlow, P. S., Moore, I. T., LeMaster, M. P., & Mason, R. T. (2001). Movements, mating, and dispersal of red-sided gartersnakes (*Thamnophis sirtalis parietalis*) from a communal den in Manitoba. *Copeia*, *2001*(1), 82–91. https://doi.org/10.1643/0045-8511(2001)001[0082:MMADOR]2.0.CO;2

Soltis, D. E., Gitzendanner, M. A., Strenge, D. D., & Soltis, P. S. (1997). Chloroplast DNA intraspecific phylogeography of plants from the Pacific Northwest of North America. *Plant Systematics and Evolution*, *206*(1), 353–373. https://doi.org/10.1007/BF00987957

Soltis, D. E., Morris, A. B., McLachlan, J. S., Manos, P. S., & Soltis, P. S. (2006). Comparative phylogeography of unglaciated eastern North America. *Molecular Ecology*, *15*(14), 4261–4293. https://doi.org/10.1111/j.1365-294X.2006.03061.x

Stange, M., Sánchez-Villagra, M. R., Salzburger, W., & Matschiner, M. (2018). Bayesian divergence-time estimation with genome-wide single-nucleotide polymorphism data of sea catfishes (Ariidae) supports Miocene closure of the Panamanian isthmus. *Systematic Biology*, *67*(4), 681–699. https://doi.org/10.1093/sysbio/syy006

Steele, C. A., & Storfer, A. (2006). Coalescent-based hypothesis testing supports multiple Pleistocene refugia in the Pacific Northwest for the Pacific Giant salamander (*Dicamptodon tenebrosus*). *Molecular Ecology*, *15*(9), 2477–2487. https://doi.org/10.1111/j.1365-294X.2006.02950.x

Suchard, M. A., Lemey, P., Baele, G., Ayres, D. L., Drummond, A. J., & Rambaut, A. (2018). Bayesian phylogenetic and phylodynamic data integration using BEAST 1.10. *Virus Evolution*, *4*(1), vey016.

Swenson, N. G., & Howard, D. J. (2005). Clustering of contact zones, hybrid zones, and phylogeographic breaks in North America. *The American Naturalist*, *166*(5), 581–591.

Syfert, M. M., Smith, M. J., & Coomes, D. A. (2013). The effects of sampling bias and model complexity on the predictive performance of MaxEnt species distribution models. *PLoS One*, *8*(2), e55158. https://doi.org/10.1371/journal.pone.0055158

Toews, D. P. L., Taylor, S. A., Vallender, R., Brelsford, A., Butcher, B. G., Messer, P. W., & Lovette, I. J. (2016). Plumage genes and little else distinguish the genomes of hybridizing warblers. *Current Biology*, *26*(17), 2313–2318. https://doi.org/10.1016/j.cub.2016.06.034

Uetz, P., Cherikh, S., Shea, G., Ineich, I., Campbell, P. D., Doronin, I. V., Rosado, J., Wynn, A., Tighe, K. A., & McDiarmid, R. (2019). A global catalog of primary reptile type specimens. *Zootaxa*, *4695*(5), 438–450.

Van Belleghem, S. M., Baquero, M., Papa, R., Camilo Salazar, W., McMillan, O., Counterman, B. A., Jiggins, C. D., & Martin, S. H. (2018). Patterns of Z chromosome divergence among *Heliconius* species highlight the importance of historical demography. *Molecular Ecology*, *27*(19), 3852–3872. https://doi.org/10.1111/mec.14560

Vicoso, B., Emerson, J. J., Zektser, Y., Mahajan, S., & Bachtrog, D. (2013). Comparative sex chromosome genomics in snakes: Differentiation, evolutionary strata, and lack of global dosage compensation. *PLoS Biology*, *11*(8), e1001643. https://doi.org/10.1371/journal.pbio.1001643

Warren, D. L., Glor, R. E., & Turelli, M. (2008). Environmental niche equivalency versus conservatism: Quantitative approaches to niche evolution. *Evolution*, *62*(11), 2868–2883. https://doi.org/10.1111/j.1558-5646.2008.00482.x

Warren, D. L., Glor, R. E., & Turelli, M. (2010). ENMTools: A toolbox for comparative studies of environmental niche models. *Ecography*, *33*(3), 607–611. https://doi.org/10.1111/j.1600-0587.2009.06142.x

Warren, D. L., & Seifert, S. N. (2011). Ecological niche modeling in Maxent: The importance of model complexity and the performance of model selection criteria. *Ecological Applications*, *21*(2), 335–342. https://doi.org/10.1890/10-1171.1

Webb, S. D. (1990). Historical biogeography. In R. L. Myers & J. J. Ewel (Eds.), *Ecosystems of Florida* (pp. 70–100). The University of Central Florida Press.

Weir, B. S., & Clark Cockerham, C. (1984). Estimating F-statistics for the analysis of population structure. *Evolution*, *38*(6), 1358–1370. https://doi.org/10.1111/j.1558-5646.1984.tb05657.x

Wiens, J. J. (2004). Speciation and ecology revisited: Phylogenetic niche conservatism and the origin of species. *Evolution*, *58*(1), 193–197. https://doi.org/10.1111/j.0014-3820.2004.tb01586.x

Wood, D. A., Vandergast, A. G., Lemos Espinal, J. A., Fisher, R. N., & Holycross, A. T. (2011). Refugial isolation and divergence in the narrowheaded gartersnake species complex (*Thamnophis rufipunctatus*) as revealed by multilocus DNA sequence data. *Molecular Ecology*, *20*(18), 3856–3878. https://doi.org/10.1111/j.1365-294X.2011.05211.x

Wright, S. (1943). Isolation by distance. *Genetics*, *28*(2), 114–138. https://doi.org/10.1093/genetics/28.2.114

Zheng, Y., Peng, R., Kuro-o, M., & Zeng, X. (2011). Exploring patterns and extent of bias in estimating divergence time from mitochondrial DNA sequence data in a particular lineage: A case study of salamanders (order Caudata). *Molecular Biology and Evolution*, *28*(9), 2521–2535. https://doi.org/10.1093/molbev/msr072

Zink, R. M. (2002). Methods in comparative Phylogeography, and their application to studying evolution in the north American aridlands. *Integrative and Comparative Biology*, *42*(5), 953–959. https://doi.org/10.1093/icb/42.5.953

BIOSKETCHES

Leonard N. Jones II is a postdoctoral fellow in the EEB department at the University of Michigan, whose research interests reside at the intersection of phylogenetics and spatial population structure. This work extends from part of his dissertation at the University of Washington investigating spatial and temporal variation in snakes.

Adam D. Leaché is an Associate Professor of Biology and Curator of Herpetology and Genetic Resources at the Burke Museum of Natural History and Culture at the University of Washington. He studies phylogenetics, phylogeography and species delimitation.

Frank T. Burbrink is the curator of reptiles and amphibians at the American Museum of Natural History and examines population genetics, phylogeography and evolution of snakes.

Author Contributions: Leonard N. Jones II, Adam D. Leaché and Frank T. Burbrink designed the study. Leonard N. Jones II collected and processed molecular data, conducted analyses,

visualized results and wrote the manuscript with contributions from all coauthors.

SUPPORTING INFORMATION

Additional supporting information can be found online in the Supporting Information section at the end of this article.

How to cite this article: Jones, L. N. II, Leaché, A. D., & Burbrink, F. T. (2023). Biogeographic barriers and historic climate shape the phylogeography and demography of the common gartersnake. *Journal of Biogeography*, *00*, 1–18. https://doi.org/10.1111/jbi.14709